

# A Hybrid Method for Power System Frequency Estimation

Jinfeng Ren, *Student Member, IEEE*, and Mladen Kezunovic, *Fellow, IEEE*

**Abstract**—Power system frequency is a critical parameter of voltage and current measurements for many applications, such as power quality, monitoring, and protection. This paper presents a hybrid approach for frequency estimation based on Taylor series expansion and Fourier algorithm. The method is derived using a dynamic signal model with varying parameters. The changing envelope of a power signal within an observation data window is approximated with a second-order Taylor series. A Fourier algorithm-based method is proposed to compute the parameters of such signal model. The algorithm using the linear model approach aimed at alleviating the computational complexity is also presented. The comparison of the performance under various conditions between the two approaches is conducted. Inheriting from the use of Fourier algorithm, this hybrid algorithm is immune to power system harmonics. It achieves excellent performance for signals with dynamic variations. The performance is investigated and compared with other techniques through simulations for various scenarios observed in real power systems. Experimental studies demonstrate the advantages of the proposed algorithm.

**Index Terms**—Fourier algorithm, frequency estimation, power system frequency, Taylor series.

## I. INTRODUCTION

**P**OWER SYSTEM frequency as a key property of the voltages and currents is used by many applications for the purpose of monitoring, protection and control. The simplest way to estimate the frequency for a given signal is to measure the time of zero crossings. However, in reality the measured signals are usually distorted and noisy, which introduces large error to the estimate. Fourier algorithm, which has been widely used as frequency estimator due to its low computation requirement, is derived based on stationary sinusoidal signal [1]. Thus, it has difficulty in handling slowly changing signals under dynamic conditions. Besides, the implicit data window in Fourier approach causes errors when frequency deviates from its nominal value [2].

Manuscript received May 06, 2011; revised December 19, 2011; accepted February 13, 2012. Date of publication June 05, 2012; date of current version June 20, 2012. This work was supported by the National Science Foundation I/UCRC called the Power System Engineering Research Center (PSERC) under Project T-43 titled “Verifying Interoperability and Application Performance of PMUs and PMU-enabled IEDs at the Device and System Level.” Paper no. TPWRD-00376-2011.

The authors are with the Department of Electrical and Computer Engineering, Texas A&M University, College Station, TX 77843-3128 USA (e-mail: j.f.ren@neo.tamu.edu; kezunov@ece.tamu.edu).

Color versions of one or more of the figures in this paper are available online at <http://ieeexplore.ieee.org>.

Digital Object Identifier 10.1109/TPWRD.2012.2196770

Over the years, many techniques have been developed to estimate the power system frequency more accurately. Iterative approach, Kalman filter, least mean square method, improved Fourier algorithm, orthogonal filtering, Taylor series expansion approach, and wavelet method are some of well known developed techniques [2]–[18]. The method using three consecutive samples of the instantaneous input signal is discussed in [18]. Among those techniques, some require dedicated filters for removal of harmonic components contained in measured signals before applying the algorithm, thus the method accuracy mainly relies on the performance of filtering. Some methods are derived based on stationary signal model, thus they hardly meet the accuracy requirement when exposed to dynamic varying signals. Some techniques use balanced three phase signals for resolving zero-crossing issues, thus they cannot deal with unbalanced conditions. And some approaches derived based on instantaneous samples require extra effort to resolve zero-crossing issues. Intelligent techniques-based approaches (e.g., genetic algorithm [19] and neural network [20]) are employed in this area as well. Although better performance may be achieved by such optimization techniques, the implementations are more complex and computationally intensive.

This paper develops a frequency estimation method based on a dynamic signal model. Taylor series expansion is used to approximate the dynamic signal spanning observation windows using a quadratic polynomial. The parameters are computed using the method derived based on discrete Fourier algorithm. The computing method for linear approximation is derived as well to alleviate the computational complexity. Their performance under dynamic conditions is compared as well. One signal cycle plus two samples and one signal cycle plus one sample are needed for the quadratic model and linear model respectively. Comparing with the traditional Fourier algorithm, this method introduces more computational load. Nevertheless, the computation is still less complex and intensive than other techniques. This method is immune to harmonic distortions and features outstanding noise rejection. Moreover, it achieves very high accuracy for signals with dynamic variations. Various conditions observed in real power system, such as noise and harmonic contaminations, frequency drift, fault and power oscillation are simulated to study the method performance under those conditions. The comparison with other techniques is conducted as well to demonstrate the advantages of the proposed algorithm.

The paper is organized as follows. The frequency estimation method using Taylor series and Fourier algorithm is elaborated in Section II. The computing approach using simplified model is described in Section III. Section IV studies the performance

through simulations as well as the comparison with other techniques. Section V outlines the conclusions.

## II. IMPROVED FOURIER ALGORITHM

The traditional Fourier algorithm and some other techniques usually assume a pure sinusoidal signal model with constant amplitude and phase angle over the observation window expressed as

$$x(t) = A \cdot \cos(2\pi ft + \varphi) \quad (1)$$

where  $A$  is amplitude,  $\varphi$  is initial phase angle, and  $f$  is signal frequency. Over one cycle signal period  $T$ , the amplitude and angle at the center of the observation window where  $t = 0$  can be estimated using the Fourier algorithm as follows:

$$A = \sqrt{X_R^2 + X_I^2} \quad (2)$$

$$\varphi = \arctan \frac{X_I}{X_R}$$

$$X_R + jX_I = \frac{1}{T} \int_{-T/2}^{T/2} x(t) \cdot e^{-j2\pi f_0 t} dt \quad (3)$$

where  $f_0$  is the nominal frequency (60 Hz in this paper). Then the frequency can be estimated by the changing rate of phase angle (i.e.,  $f = f_0 + d\varphi/dt/2\pi$ ).

The assumption of constant parameters is not adequate for the signals measured during power system dynamic conditions. For better describing dynamic signals, a model with changing amplitude and phase angle is employed

$$x(t) = a(t) \cdot \cos[2\pi f_0 t + \varphi(t)]. \quad (4)$$

The amplitude  $a(t)$  and phase angle  $\varphi(t)$  are functions of time, whose variation patterns are determined by power system states. Designate  $\theta(t)$  as  $2\pi f_0 t + \varphi(t)$ . It should be pointed out that the changing angle  $\varphi(t)$  implicitly involves the frequency variation because the frequency is equal to rate of change of phase angle. As a result the signal frequency can be obtained by

$$f = \frac{\theta'(t)}{2\pi} = f_0 + \frac{\varphi'(t)}{2\pi}. \quad (5)$$

Rewrite (4) according to trigonometric function

$$x(t) = f_c(t) \cdot \cos(2\pi f_0 t) - f_s(t) \cdot \sin(2\pi f_0 t) \quad (6)$$

where  $f_c(t) = a(t) \cdot \cos[\varphi(t)]$ ,  $f_s(t) = a(t) \cdot \sin[\varphi(t)]$ . One can see that the coefficient functions  $f_c(t)$  and  $f_s(t)$  describe the envelope of the slowly changing sinusoid. Letting us expand coefficient functions with the second-order Taylor series at the center of the data window  $t = 0$ , we have

$$\begin{aligned} f_c(t) &\cong c_0 + c_1 t + c_2 t^2 \\ f_s(t) &\cong s_0 + s_1 t + s_2 t^2 \end{aligned} \quad (7)$$

where  $c_0 = f_c(0)$ ,  $c_1 = df_c(t)/dt|_{t=0}$ ,  $c_2 = d^2 f_c(t)/dt^2|_{t=0}$ ,  $s_0 = f_s(0)$ ,  $s_1 = df_s(t)/dt|_{t=0}$ , and  $s_2 = d^2 f_s(t)/dt^2|_{t=0}$ .

From (6) and (7), we have the following expression at  $t = 0$ :

$$a(0) \cos[\varphi(0)] = c_0, \quad a(0) \sin[\varphi(0)] = s_0. \quad (8)$$

We obtain the amplitude and phase angle at the center of the data window as follows:

$$\begin{aligned} A_m &= a(0) = \sqrt{c_0^2 + s_0^2} \\ \varphi_m &= \varphi(0) = \arctan \left( \frac{s_0}{c_0} \right). \end{aligned} \quad (9)$$

Taking the first derivative on both sides of (7), at  $t = 0$ , we have

$$a'(0) \cos[\varphi(0)] - a(0) \varphi'(0) \sin[\varphi(0)] = c_1 \quad (10a)$$

$$a'(0) \sin[\varphi(0)] + a(0) \varphi'(0) \cos[\varphi(0)] = s_1. \quad (10b)$$

Substituting (8) into (10a) and (10b), and eliminating  $a'(0)$ , we obtain

$$\varphi'(0) = \frac{c_0 s_1 - s_0 c_1}{c_0^2 + s_0^2}. \quad (11)$$

Suppose that the coefficients of the above quadratics are known. From (5) and (11), we derive the formula for computing the frequency

$$f = f_0 + \frac{1}{2\pi} \cdot \frac{c_0 s_1 - s_0 c_1}{c_0^2 + s_0^2}. \quad (12)$$

The amplitude and phase angle over the observation window can be calculated as well using (9). Next, we will discuss how to estimate those coefficients using the Fourier algorithm.

Let assume the sampling frequency is  $f_s = N \cdot f_0$ ,  $N$  is a positive integer, then the sampling interval is  $\Delta t = 1/f_s$ . Apply the discrete Fourier transform to signal  $x(k)$  ( $k$  is an integer) over one cycle period from  $-N/2 + 1$  to  $N/2$  ( $N$  is even), or from  $-(N-1)/2$  to  $(N-1)/2$  ( $N$  is odd). For simplicity, let us neglect the multiple  $2/N$  and  $\Delta t$ , and denoting the real part and imaginary part as  $X_R$  and  $X_I$ , we have

$$F_{x(k)} = \sum_{k=-N/2+1}^{N/2} x(k) \cdot e^{-j(2\pi k/N)} = X_R + jX_I. \quad (13)$$

Substitute  $x(k)$  with (6) in discrete form, and  $e^{-j2\pi k/N}$  with  $\cos(2\pi k/N) - j \cdot \sin(2\pi k/N)$ . The left-hand side can be written as

$$\begin{aligned} &\sum_{k=-N/2+1}^{N/2} [c_0 + c_1 k \Delta t + c_2 (k \Delta t)^2] \cdot \cos^2 \left( \frac{2\pi k}{N} \right) \\ &- [s_0 + s_1 k \Delta t + s_2 (k \Delta t)^2] \cdot \sin \left( \frac{2\pi k}{N} \right) \cos \left( \frac{2\pi k}{N} \right) \\ &- j [c_0 + c_1 k \Delta t + c_2 (k \Delta t)^2] \cdot \cos \left( \frac{2\pi k}{N} \right) \sin \left( \frac{2\pi k}{N} \right) \\ &+ j [s_0 + s_1 k \Delta t + s_2 (k \Delta t)^2] \cdot \sin^2 \left( \frac{2\pi k}{N} \right). \end{aligned} \quad (14)$$

Arranging the real part and imaginary part, we have

$$\alpha_0 c_0 + \gamma_0 c_0 + \alpha_1 c_1 + \gamma_1 s_1 + \alpha_2 c_2 + \lambda_2 s_2 = X_R \quad (15a)$$

$$\gamma_0 c_0 + \beta_0 s_0 + \gamma_1 c_1 + \beta_1 s_1 + \gamma_2 c_2 + \beta_2 s_2 = X_I. \quad (15b)$$

The expressions for coefficients  $\alpha_0$ ,  $\alpha_1$ ,  $\alpha_2$ ,  $\beta_0$ ,  $\beta_1$ ,  $\beta_2$ ,  $\gamma_0$ ,  $\gamma_1$ , and  $\gamma_2$  are given in the Appendix.

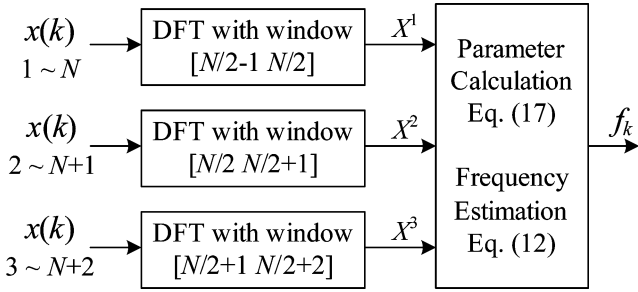


Fig. 1. Block diagram of the frequency estimation algorithm.

One can see from (15a) and (15b) that there are six unknown variables with two equations. To solve the variables, let us obtain four more equations by applying DFT to  $x(k)$  over the window  $[-N/2N/2 + 1]$  and  $[-N/2 + 1N/2 + 2]$  ( $N$  is even), respectively. Letting us mark the three DFTs with superscripts 1, 2, and 3, and rewriting them in matrix form, we have

$$\begin{bmatrix} \alpha_0^1 & \gamma_0^1 & \alpha_1^1 & \gamma_1^1 & \alpha_2^1 & \gamma_2^1 \\ \gamma_0^1 & \beta_0^1 & \gamma_1^1 & \beta_1^1 & \gamma_2^1 & \beta_2^1 \\ \alpha_0^2 & \gamma_0^2 & \alpha_2^2 & \gamma_2^2 & \alpha_3^2 & \gamma_3^2 \\ \gamma_0^2 & \beta_0^2 & \gamma_2^2 & \beta_2^2 & \gamma_3^2 & \beta_3^2 \\ \alpha_0^3 & \gamma_0^3 & \alpha_3^3 & \gamma_3^3 & \alpha_2^3 & \gamma_2^3 \\ \gamma_0^3 & \beta_0^3 & \gamma_2^3 & \beta_2^3 & \gamma_3^3 & \beta_3^3 \end{bmatrix} \cdot \begin{bmatrix} c_0 \\ s_0 \\ c_1 \\ s_1 \\ c_2 \\ s_2 \end{bmatrix} = \begin{bmatrix} X_R^1 \\ X_I^1 \\ X_R^2 \\ X_I^2 \\ X_R^3 \\ X_I^3 \end{bmatrix}. \quad (16)$$

Denoting  $H$  as the coefficient matrix,  $V = [c_0 \ s_0 \ c_1 \ s_1 \ c_2 \ s_2]^T$  and  $X = [X_R^1 \ X_I^1 \ X_R^2 \ X_I^2 \ X_R^3 \ X_I^3]^T$ , we have  $H \cdot V = X$ . In (16), the coefficient matrix  $H$  can be calculated in advance. We utilize the matrix computation technique to decompose  $H$  into  $L$  and the  $U$  matrix for the demand of fast computing. To obtain the DFT vector  $X$ ,  $N + 2$  samples of input signal  $x(k)$  are required. The overall computation load for solving the variables is approximately  $6N + 62$  multiplications and  $6N + 30$  summations, which is far less compared to other methods. The computing burden can be reduced further by using the recursive Fourier technique [21], [22]. Performing the matrix operation, the estimated frequency can be computed using (12). The block diagram of the algorithm is given in Fig. 1.

### III. SIMPLIFIED APPROACH

For some conditions, for example, the low frequency oscillation, the amplitude, and phase angle within an observation window are varying slowly. In this case, the signal envelope can be represented linearly. Rewrite (6) as

$$x(t) \cong (c_0 + c_1 t) \cos(2\pi f_0 t) - (s_0 + s_1 t) \sin(2\pi f_0 t). \quad (17)$$

One can see that the number of variables is reduced to four. Thus,  $N + 1$  samples of the input signal  $x(k)$  are used for two times of DFT over window  $[-N/2 + 1 \ N/2]$  and

$[N/2 \ N/2 + 1]$ , respectively. The corresponding matrix is given as

$$\begin{bmatrix} \alpha_0^1 & \gamma_0^1 & \alpha_1^1 & \gamma_1^1 \\ \gamma_0^1 & \beta_0^1 & \gamma_1^1 & \beta_1^1 \\ \alpha_0^2 & \gamma_0^2 & \alpha_1^2 & \gamma_1^2 \\ \gamma_0^2 & \beta_0^2 & \gamma_1^2 & \beta_1^2 \end{bmatrix} \cdot \begin{bmatrix} c_0 \\ s_0 \\ c_1 \\ s_1 \end{bmatrix} = \begin{bmatrix} X_R^1 \\ X_I^1 \\ X_R^2 \\ X_I^2 \end{bmatrix}. \quad (18)$$

The linear coefficients can be obtained by solving matrix (18). Similarly, the frequency can be estimated by (12). For the linear model, the computation burden can be significantly reduced. The comparison between the linear model and quadratic model will be studied next. Simulation studies show that the linear approximation under the slowly changing condition is adequate.

### IV. SIMULATION STUDIES

Numerous simulation experiments using various types of signals that can be observed from the real power system are presented in this section. The test signals represent different operating conditions of a power system including noise and harmonic contaminations, frequency drift, and power oscillation. The proposed hybrid technique for frequency estimation using the quadratic model and linear model, denoted as HB2 and HB1, respectively, is tested using simulation. A comparison of the results with a newly developed sample-based technique (denoted as SBT) in [18] is presented to demonstrate the merit of the proposed method.

For implementing the algorithm SBT, HB1 and HB2, the test signals are sampled at 960 Hz ( $N = 16$ ), which is the sampling frequency mainly used by most intelligent electronic devices (IEDs) in substations. As required by the SBT algorithm, an FIR band-pass filter with order 32 is applied to input signals when handling the signals in the presence of white noise and harmonics. The frequency response of the BP filter is shown in Fig. 2.

#### A. In the Presence of Harmonics

Let us use the power signals contaminated with different orders of harmonics, which is expressed as follows:

$$x(t) = A_0 \cdot \cos(2\pi f_0 t + \varphi_0) + A_i \cdot \cos(2\pi f_i t + \varphi_i) \quad (19)$$

where  $A_0$ ,  $f_0$ , and  $\varphi_0$  are the amplitude, frequency, and initial angle of the nominal frequency signal while  $A_i$ ,  $f_i$ , and  $\varphi_i$  are the parameters for harmonic components.

Consider the order of harmonics up to eight (2nd 3rd...8th) and set their magnitudes to 50%, 33%, 25%, 20%, 16%, 14%, and 12%, respectively. Fig. 3 shows the distorted input signal containing the third-order harmonic. The corresponding frequency estimates computed by the three algorithms are given in Fig. 4. The estimation errors are calculated by taking the mean over 0.1 s period of input signals. The results by three algorithms for each harmonic contamination case are summarized in Table I. As expected, the proposed method is immune

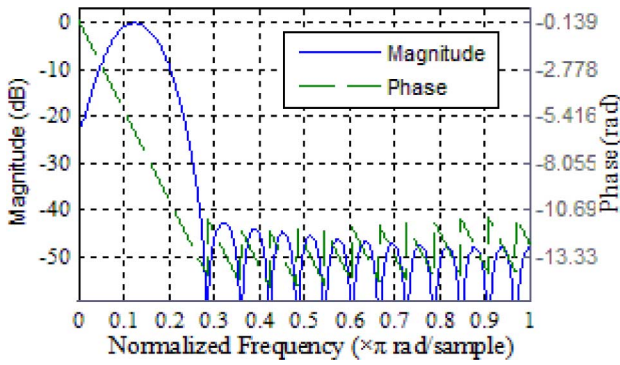


Fig. 2. Frequency response of the FIR band-pass filter.

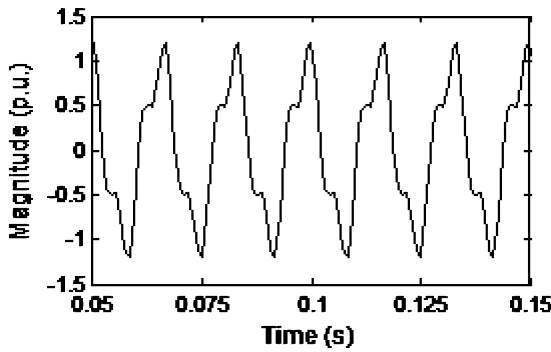


Fig. 3. Input signal containing the third-order harmonic.

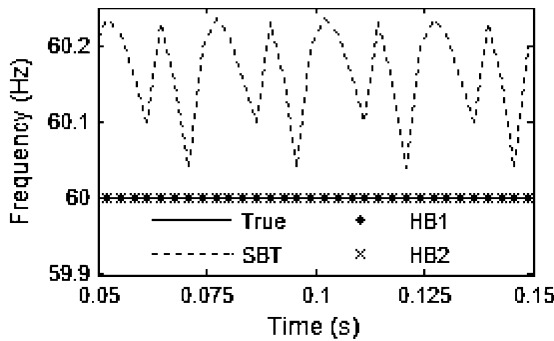


Fig. 4. Output frequency estimates by three algorithms.

to harmonic contamination. Using a well-designed BP filter may help improve the accuracy of the SBT algorithm.

**B. Noise Rejection Test**

The capability of the noise rejection of the frequency estimation techniques is investigated using the sinusoidal signal described in (1) superimposed with zero-mean Gaussian noise. The white noise with various signal-to-noise ratios (SNRs) (e.g., 40, 50, 70, and 80 dB) are added to the test signals. Since the noise signals are generated randomly, the algorithms are performed 100 times and the mean value of the estimated frequency error (in hertz) is computed for each noise level. The results for algorithm HB1 and HB 2 are given in Fig. 5 with comparison to the SBT algorithm. The estimation errors are summarized in Table II. As expected, the instantaneous sample-based method is

TABLE I  
ESTIMATION ERRORS IN THE PRESENCE OF HARMONICS

Harmonics	Frequency Estimation Error (Hz)		
	SBT	HB1	HB2
2nd	4.64e-001	1.90e-013	3.89e-014
3rd	1.65e-001	2.39e-013	4.22e-014
4th	5.06e-002	1.74e-013	4.46e-014
5th	4.82e-001	2.16e-013	4.17e-014
6th	4.90e-002	2.29e-013	4.44e-014
7th	2.33e-001	2.53e-013	4.34e-014
8th	7.31e-002	1.57e-013	3.31e-014

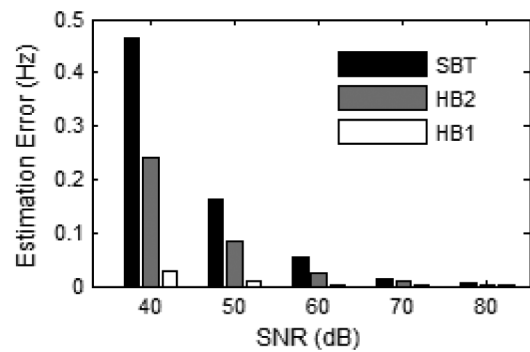


Fig. 5. Estimated frequency errors in the presence of noise.

TABLE II  
ESTIMATION ERRORS IN THE PRESENCE OF NOISE

Noise Level (dB)	Frequency Estimation Error (mHz)		
	SBT	HB2	HB1
40	538.29	224.51	26.96
50	177.10	79.36	8.54
60	59.28	25.69	2.60
70	16.34	8.43	0.89
80	6.24	2.42	0.24

sensitive to noise. HB1 exhibits better noise rejection than HB2. This may result from the reduced computational complexity.

**C. Frequency Ramp**

In this section, the performance of the proposed algorithms exposed to signals with a linear variation of frequency is investigated. Consider the rate of change of frequency  $df = \pm 1$  Hz. The signal frequency varies from its nominal value for 2 s, that is, increasing from 60 to 62 Hz for the positive rate of change and decreasing from 60 to 58 Hz for the negative rate of change. The responses of the proposed methods HB1 and HB2 are also compared to the response of SBT. Figs. 6 and 7 show their responses at the beginning of the ramp (around 0.2 s) and at the end (around 2 s) for the positive and negative rate of change, respectively. As we can observe, the frequency outputs estimated

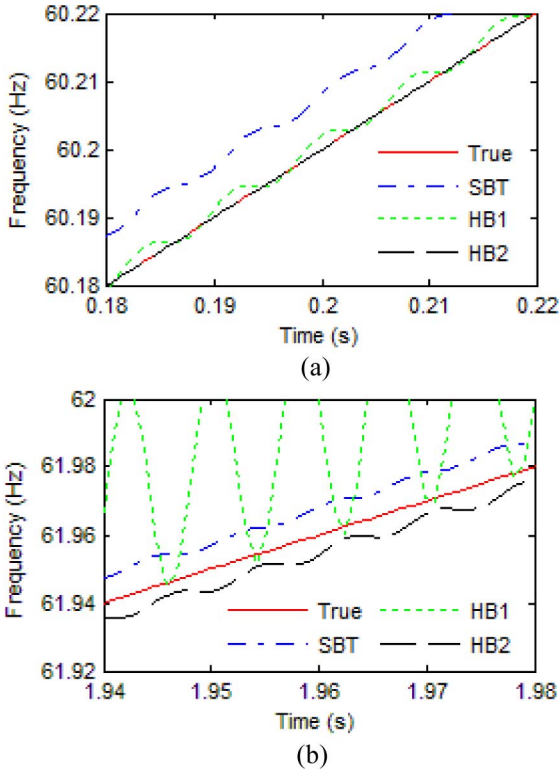


Fig. 6. Responses for  $df = 1$  Hz. (a) At the beginning of the frequency ramp. (b) At the end of the frequency ramp.

by the HB2 method follow the inputs very close. From Figs. 6(a) and (7a), we can observe that HB1 achieves better accuracy than SBT. As the frequency deviates from its nominal value, HB1 has fairly large errors, as shown in Figs. 6(b) and 7(b). This is caused by the linear approximation.

#### D. Modulated Frequency

In power system modulations, amplitude and phase angle occur when the balance of power generation and consumption gets violated due to system disturbances, such as a fault or loss of load. This phenomenon involves electromechanical transients, which may cause frequency fluctuations, particularly the phase modulation. Considering that the frequency varies as a sinusoid, we use the following model to generate input signals:

$$x(t) = A_0 \cdot \cos[2\pi f_0 t + \varphi_0 + A_f \cos(2\pi f_m t + \varphi_f)] \quad (20)$$

where  $f_m$  is the modulation frequency.  $A_f$  and  $\varphi_f$  are the amplitude and initial phase angle. Then, the real frequency can be expressed as

$$f(t) = f_0 - A_f \cdot f_m \cdot \sin(2\pi f_m t + \varphi_f). \quad (21)$$

Let  $A_f = 0.2$  p.u., and  $f_m$  vary from 0.1 to 5 Hz. The accuracy of HB1 and HB2 is compared with SBT. The average frequency estimation errors over one cycle period corresponding to modulation frequency are calculated and shown in Table III. Simulation results indicate that the frequency estimates by the three algorithms follow the inputs very close under slowly changing conditions. Fig. 8 gives the responses of the

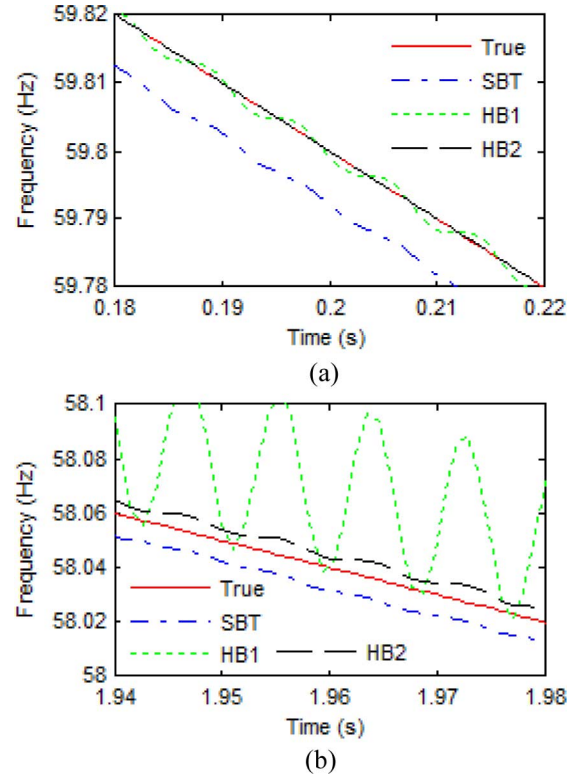


Fig. 7. Responses for  $df = -1$  Hz. (a) At the beginning of the frequency ramp. (b) At the end of the frequency ramp.

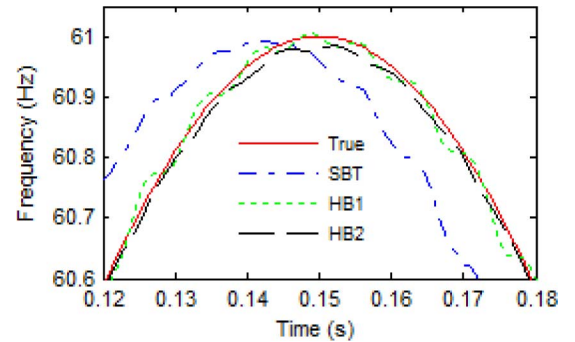


Fig. 8. Frequency responses of three algorithms under  $f_m = 5$  Hz.

TABLE III  
ESTIMATION ERRORS FOR MODULATED FREQUENCY

Modulation Frequency (Hz)	Frequency Estimation Error (Hz)		
	SBT	HB1	HB2
0.1	5.84e-05	8.03e-06	8.57e-08
0.5	1.38e-03	1.92e-04	1.14e-05
1.0	5.79e-03	8.05e-04	8.62e-05
5.0	1.45e-01	2.19e-02	1.05e-02

three algorithms exposed to the signals modulated with 5 Hz. The results demonstrate that the linear model is adequate for slowly changing signals while the quadratic model is capable of tracking fast changing signals.

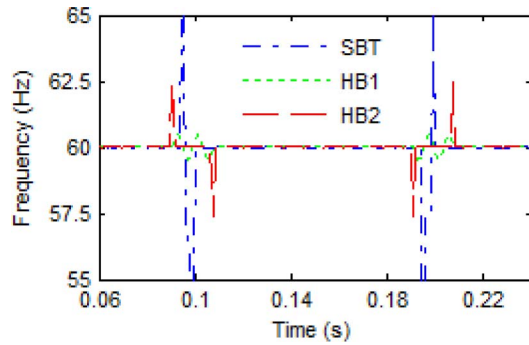


Fig. 9. Dynamic responses of three algorithms for amplitude steps.

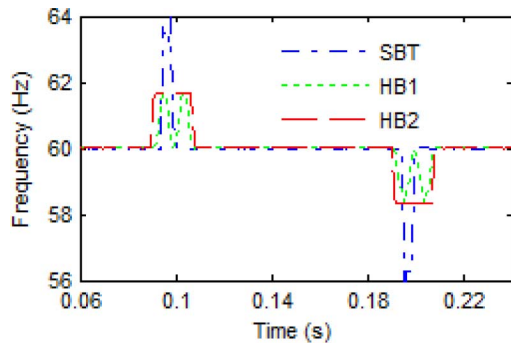


Fig. 10. Dynamic responses of three algorithms for phase-angle steps.

### E. Steps in Amplitude, Phase, and Frequency

Faults and switching operations in power systems may cause abrupt changes in the amplitude and phase angle of the voltage and current waveforms. Some other disturbances, such as generation tripping, may result in frequency jumps. In this section, we study the dynamic behavior of the hybrid algorithms HB1 and HB2 using step signals as specified in IEEE standard C37.118 [23]. Their responses are also compared with SBT. A test signal with  $-10\%$  step in amplitude at 0.1 s followed by reversing the amplitude back to the starting value at 0.2 s is fed to the algorithms. Their responses are shown in Fig. 9.

As expected, the frequency estimators suffer a transition during the amplitude step. The response time depends on the length of the data window that the estimators use for computation. One can see that SBT has the shortest response period. However, it has difficulty in handling the harmonics and noise. Although the proposed methods require a longer settling period, they achieve good accuracy over distorted signals. It has to be pointed out that the half cycle plus one or two samples can be used for HB1 and HB2 to gain faster response for dynamic signals, whereas the accuracy will be affected by the signals containing even-order harmonics. Similar to the amplitude step, a test signal with  $\pm\pi/10$  phase angle step at 0.1 and 0.2 s, respectively, is fed to the frequency estimators. Fig. 10 shows their behavior which is similar to the result of the amplitude step.

For the frequency jump, signals with  $\pm 1$  Hz variation steps from the nominal value 60 Hz are used to observe the dynamic behavior of the methods. Figs. 11 and 12 show their responses for the positive and negative steps, respectively. All of the

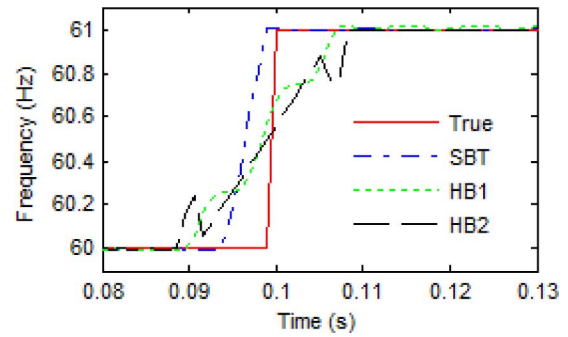


Fig. 11. Dynamic responses of three algorithms for +1 Hz frequency step.

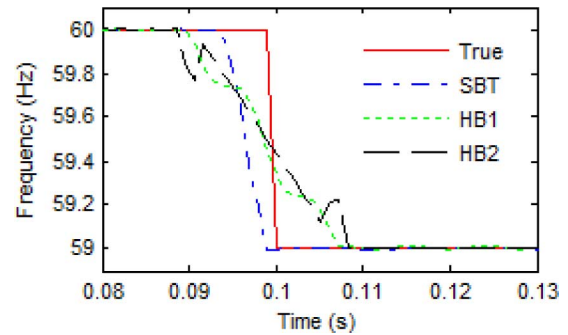
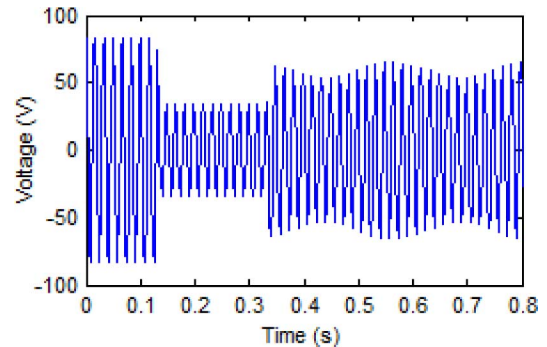
Fig. 12. Dynamic responses of three algorithms for  $-1$  Hz frequency step.

Fig. 13. Voltage waveforms for the first case.

methods under test exhibit smooth transitions during steps. As expected, SBT responses are fast because of the shortest data window.

### F. Transient Signals

The voltage signals generated from the time domain program ATP/EMTP are used to evaluate the performance of the new frequency estimation algorithm under transient conditions. The power system model is a 230 kV power network created by a Working Group within the IEEE Power and Energy Society's Power System Relaying Committee (PSRC) [24]. The recordings of voltage and current waveforms are imported and fed to the frequency estimation algorithms. Two scenarios are considered: one is a transmission line fault followed by tripping of a faulted line that caused power swing; another is an out of step due to a loss of load. Fig. 13 shows the secondary voltage of the faulted phase for the first case. The frequency estimates obtained by the three algorithms under this condition are given

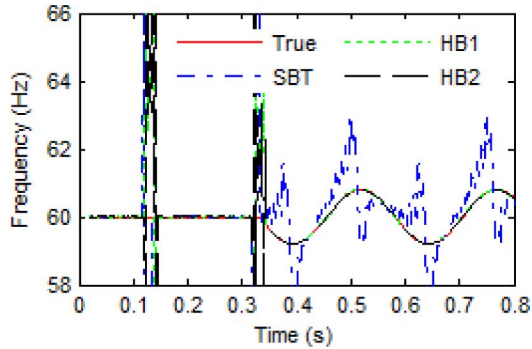


Fig. 14. Frequency responses of three algorithms for the first case.

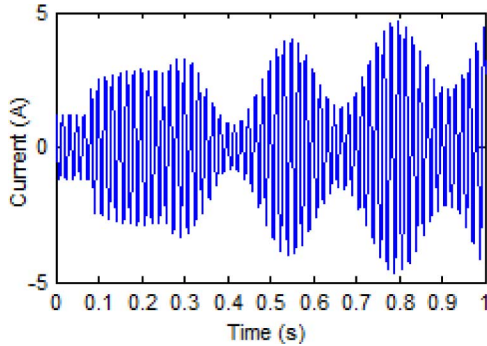


Fig. 15. Current waveforms for the second case.

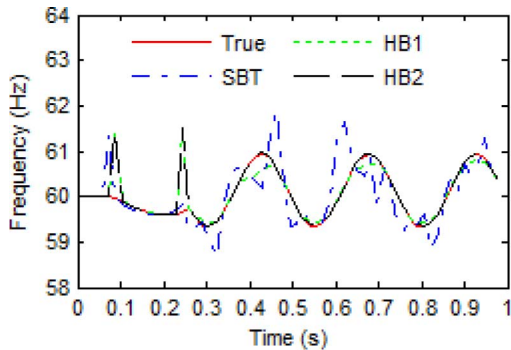


Fig. 16. Frequency responses of three algorithms for the second case.

in Fig. 14. One can observe that the methods suffer transitions during abrupt changes as expected. The accuracy of SBT is affected by the oscillation. The proposed methods HB1 and HB2 follow the frequency variation very close. For the second case, we estimate the frequency using current signals, which is shown in Fig. 15. The magnitude envelope is increasing due to the out of step. The frequency oscillates because the varying phase angle after occurrence of the out of step. Fig. 16 shows the frequency responses of the estimators. One can see that the oscillation severely affects the accuracy of SBT, whereas HB1 and HB2 are capable of following the frequency variation during power oscillations.

### G. Laboratory Experiments

In this section, we use signals collected from a digital fault recorder (DFR) to evaluate the performance of the proposed algorithm. The DFR is a part of the laboratory setup developed

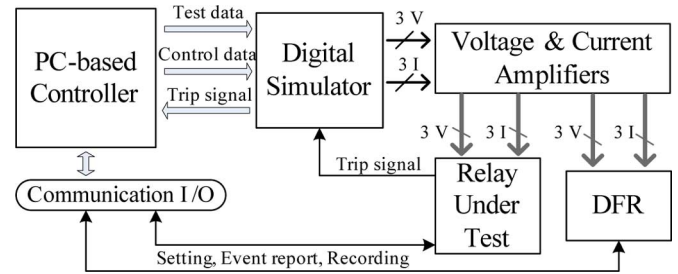


Fig. 17. Diagram of the laboratory setup for protective relay testing.

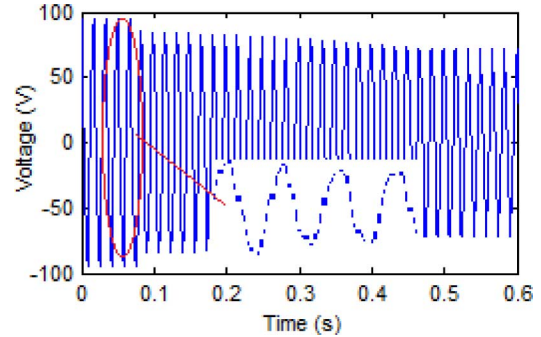


Fig. 18. Diagram of the laboratory setup for protective relay testing.

for protective relay testing [25]. Fig. 17 shows the diagram for the relay test system. It includes a PC-based controller to run associated software, a digital simulator, and a set of amplifiers used to generate voltage and current signals at nominal level, a protective relay under test, and a DFR used to record the disturbance waveforms.

The voltage and current signals retrieved from the DFR contain errors brought by the digital-to-analog converter, amplifier, and instrument transformer. Those errors may include white noise, signal distortion, and high frequency components. The sampling frequency for this DFR is 10 kHz. We retrieved voltage waveforms under an event triggered by a three-phase fault and fed them to the frequency estimators. A segment of one phase voltage containing fault data is shown in Fig. 18. The performance of the three methods is shown in Fig. 19. One can see that the performance of SBT is affected by the dynamic signal itself and the contaminating components while the HB1 and HB2 exhibit the same accuracy for the slowly changing inputs.

## V. CONCLUSIONS

A hybrid method for real-time frequency estimation based on Taylor series and a discrete Fourier algorithm is proposed in this paper. Two approaches using the quadratic model and linear model are presented to achieve better accuracy and less computational complexity, respectively. The performance of the proposed methods is compared to an instantaneous sample-based technique. The conclusions are as follows.

- The new techniques achieve high harmonics and noise rejection.
- The approach using the quadratic model achieves high accuracy under dynamic conditions.

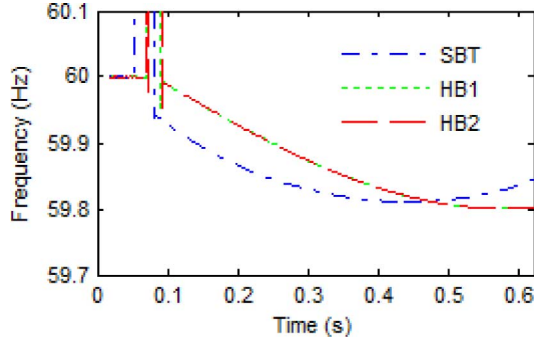


Fig. 19. Diagram of the laboratory setup for protective relay testing.

- The simplified method using linear approximation is adequate for slowly changing signals. It features better noise rejection compared to the quadratic model approach.
- Frequency estimates computed over the data window containing abrupt changes in amplitude, phase angle, and frequency may be invalid. Such measurements need to be marked as bad measurements for the frequency-critical applications.
- The sampling frequency required by the proposed algorithm is in a prevailing range, and the computation burden is low. This method can be used for real-time power system frequency tracking.

#### APPENDIX

The coefficients in (15a) and (15b) are

$$\begin{aligned}
 \alpha_0 &= \sum_{-N/2+1}^{N/2} \cos^2\left(\frac{2\pi k}{N}\right) \\
 \alpha_1 &= \sum_{-N/2+1}^{N/2} k\Delta t \cdot \cos^2\left(\frac{2\pi k}{N}\right) \\
 \alpha_2 &= \sum_{-N/2+1}^{N/2} (k\Delta t)^2 \cdot \cos^2\left(\frac{2\pi k}{N}\right) \\
 \beta_0 &= \sum_{-N/2+1}^{N/2} \sin^2\left(\frac{2\pi k}{N}\right) \\
 \beta_1 &= \sum_{-N/2+1}^{N/2} k\Delta t \cdot \sin^2\left(\frac{2\pi k}{N}\right) \\
 \beta_2 &= \sum_{-N/2+1}^{N/2} (k\Delta t)^2 \cdot \sin^2\left(\frac{2\pi k}{N}\right) \\
 \gamma_1 &= -\frac{1}{2} \cdot \sum_{-N/2+1}^{N/2} k\Delta t \cdot \sin\left(\frac{4\pi k}{N}\right). \quad (22)
 \end{aligned}$$

#### REFERENCES

- [1] A. G. Phadke, J. Thorp, and M. Adamiak, "A new measurement technique for tracking voltage phasors, local system frequency and rate of change of frequency," *IEEE Trans. Power App. Syst.*, vol. PAS-102, no. 5, pp. 1025–1038, May 1983.
- [2] T. S. Sidhu and M. S. Sachdev, "An iterative technique for fast and accurate measurement of power system frequency," *IEEE Trans. Power Del.*, vol. 13, no. 1, pp. 109–115, Jan. 1998.

- [3] V. V. Terzija, M. B. Djuric, and B. D. Kovacevic, "Voltage phasor and local system frequency estimation using Newton type algorithm," *IEEE Trans. Power Del.*, vol. 9, no. 3, pp. 1368–1374, Jul. 1994.
- [4] P. K. Dash, A. K. Pradhan, and G. Panda, "Frequency estimation of distorted power system signals using extended complex Kalman filter," *IEEE Trans. Power Del.*, vol. 14, no. 3, pp. 761–766, Jul. 1999.
- [5] A. Routray, A. K. Pradhan, and K. P. Rao, "A novel Kalman filter for frequency estimation of distorted signals in power systems," *IEEE Trans. Instrum. Meas.*, vol. 51, no. 3, pp. 469–479, Jun. 2002.
- [6] A. A. Girgis and W. L. Peterson, "Adaptive estimation of power system frequency deviation and its rate of change for calculating sudden power system overloads," *IEEE Trans. Power Del.*, vol. 5, no. 2, pp. 585–594, Apr. 1990.
- [7] A. K. Pradhan, A. Routray, and A. Basak, "Power system frequency estimation using least mean square technique," *IEEE Trans. Power Del.*, vol. 20, no. 3, pp. 1812–1816, Jul. 2005.
- [8] D. Barbosa, R. M. Monaro, D. V. Coury, and M. Oleskovicz, "A modified least mean square algorithm for adaptive frequency estimation in power systems," presented at the IEEE Power Energy Soc. Gen. Meeting, Pittsburgh, PA, Jul. 2008.
- [9] M. B. Djuric and Z. R. Djuric, "Frequency measurement of distorted signals using Fourier and zero crossing techniques," *Elect. Power Syst. Res.*, vol. 78, pp. 1407–1415, 2008.
- [10] M. D. Kusljevic, J. J. Tomic, and L. D. Jovanovic, "Frequency estimation of three-phase power system using weighted least square algorithm and adaptive FIR-filtering," *IEEE Trans. Instrum. Meas.*, vol. 59, no. 2, pp. 322–329, Feb. 2010.
- [11] I. Kamwa and R. Grondin, "Fast adaptive schemes for tracking voltage phasor and local frequency in power transmission and distribution systems," in *Proc. IEEE Power Eng. Soc. Transm. Distrib. Conf.*, Dallas, TX, 1991, pp. 930–936.
- [12] D. Hart, D. Novosel, Y. Hu, B. Smith, and M. Egolf, "A new frequency tracking and phasor estimation algorithm for generator protection," *IEEE Trans. Power Del.*, vol. 12, no. 3, pp. 1064–1073, Jul. 1997.
- [13] J. Szafran and W. Rebizant, "Power system frequency estimation," *Proc. Inst. Elect. Eng., Gen. Transm. Distrib.*, vol. 145, no. 5, pp. 578–582, Sep. 1998.
- [14] M. Kezunovic, P. Spasojevic, and B. Perunicic, "New digital signal processing algorithms for frequency deviation measurements," *IEEE Trans. Power Del.*, vol. 7, no. 3, pp. 1563–1573, Jul. 1992.
- [15] J. Ren and M. Kezunovic, "Real time power system frequency and phasor estimation scheme using recursive wavelet transform," *IEEE Trans. Power Del.*, vol. 26, no. 3, pp. 1392–1402, Jul. 2011.
- [16] J. Ren and M. Kezunovic, "Use of recursive wavelet transform for estimating power system frequency and phasors," presented at the IEEE Power Energy Soc. Transm. Distrib. Conf. Expo., New Orleans, LA, Apr. 2010.
- [17] P. J. Moore, J. H. Allmeling, and A. T. Johns, "Frequency relaying based on instantaneous frequency measurement," *IEEE Trans. Power Del.*, vol. 11, no. 4, pp. 1737–1742, Oct. 1996.
- [18] A. Lopez, J. C. Montano, M. Castilla, J. Gutierrez, M. D. Borrás, and J. C. Bravo, "Power system frequency measurement under nonstationary situations," *IEEE Trans. Power Del.*, vol. 23, no. 2, pp. 562–567, Apr. 2008.
- [19] K. M. El-Naggar and H. K. M. Youssef, "A genetic based algorithm for frequency relaying applications," *Elect. Power Syst. Res.*, vol. 55, no. 3, pp. 173–178, 2000.
- [20] L. L. Lai and W. L. Chan, "Real time frequency and harmonic evaluation using artificial networks," *IEEE Trans. Power Del.*, vol. 14, no. 1, pp. 52–57, Jan. 1999.
- [21] J. Yang and C. Liu, "A precise calculation of power system frequency," *IEEE Trans. Power Del.*, vol. 16, no. 3, pp. 361–366, Jul. 2001.
- [22] H. Darwish and M. Fikri, "Practical considerations for recursive DFT implementation in numerical relays," *IEEE Trans. Power Del.*, vol. 22, no. 1, pp. 42–49, Jan. 2007.
- [23] *IEEE Standard for Synchrophasors for Power Systems*, IEEE Standard C37.118-2005, Mar. 2006.
- [24] Power System Relaying Committee, EMTP reference models for transmission line relay testing report, 2004. [Online]. Available: <http://www.pes-psrc.org>
- [25] M. Kezunovic and J. Ren, "New test methodology for evaluating protective relay security and dependability," presented at the IEEE Power Energy Soc. Gen. Meeting, Pittsburgh, PA, Jul. 2008.

**Jinfeng Ren** (S'07), photograph and biography not available at the time of publication.

**Mladen Kezunovic** (S'77–M'80–SM'85–F'99), photograph and biography not available at the time of publication.